INTERNATIONAL JOURNAL OF MULTIDISCIPLINARY RESEARCH AND ANALYSIS

ISSN(print): 2643-9840, ISSN(online): 2643-9875

Volume 06 Issue 10 October 2023

DOI: 10.47191/ijmra/v6-i10-37, Impact Factor: 7.022

Page No. 4828-4841

Enhancement of Power Systems Transient Stability with TCSC: A Case study of The Nigerian 330 kV, 48-Bus Network

Imo E. Nkan[1], Ekom E. Okpo[1], Aniekan B. Inyang[2]

[1]Department of Electrical and Electronic Engineering, Akwa Ibom State University Ikot Akpaden, Nigeria.

[2]Department of Electrical/Electronic Engineering Technology, Akwa Ibom State Polytechnic Ikot Osurua, Nigeria.

ABSTRACT: A steady, safe, controllable, and high-quality power supply is necessary given the complexity of power systems, especially in the deregulated power sector seen in Nigeria. One of the main drawbacks of network expansion is the loss of the system's overall damping torque, which mitigates the system resulting to fluctuations and transient instability. Power system stability control difficulties have been addressed using flexible AC transmission systems (FACTS) controllers. This study examines the responses of the generator rotor angle, speed, Q-axis and D-axis voltage components behind transient reactance as well as the voltage magnitude profile under the influence of a three-phase fault for the purpose of enhancing transient stability. The Nigerian 48-bus power system network was modeled using commercial PSAT software in a MATLAB environment with a fault induced on Bus 33 (Geregu SubStation) and TCSC optimally positioned on line 21-28 using continuation power flow (CPF). According to simulation results with and without TCSC, a significant amount of oscillation in the power system was dampened, and the voltage profile was improved for power system transient stability.

KEYWORDS: transient stability, TCSC, FACTS, rotor angle, Q-axis, D-axis, PSAT, continuation power flow

I. INTRODUCTION

In the field of electric energy, the role of the electric network is crucial. Physical laws dictate how it functions. Different voltage levels make up the fixed structure of the electric network; the higher levels are used for transmission, while the lower levels are employed for distribution. The amount of electricity that can be transferred or distributed is constrained by the finite capacity of each network component. Because of the considerably stricter cost restrictions than in the past, the network operator is most concerned with making efficient use of all network components. It is clear that the cost limits significantly increase operational complexity given that operating a large electric network is a complex and difficult engineering endeavor. More flexibility is needed in terms of cross-border trading of electricity as the interconnected network grows larger. Due to issues with voltage, angle, and frequency stability, operational issues also become more difficult at the same time. Power system stability is the capacity of an electric power system, given a specific initial operating condition, to return to a state of operating equilibrium after being subjected to a physical disturbance, with most system variables bound so that essentially the entire system stays intact. In terms of voltage stability, this refers to a power system's capacity to sustain a reasonable level of power across all of its buses both under normal circumstances and following a disturbance in the power network. Therefore, a deviation from the old methods of power system generation, distribution, control, and security has necessitated the application of FACTS controllers and in this case, TCSC for power utilization of existing power systems (Hingorani, 2000).

II. REVIEW OF RELATED LITERATURE

The ability of power systems to maintain synchronous operation and continuous delivery of electric power after unexpected disturbances is pertinent. This necessitate extensive research into novel strategies to mitigate transient instability in power systems. Thyristors-Controlled Series Compensators (TCSC) offers a promising solution by dynamically regulating reactance to enhance voltage control and power transmission during transient faults. The studies in (Sunikumar, 2012; Nkan, Okoro, Obi, Awah, & Akuru, 2019; Karthiga, Raja, & Venkatesh, 2017; Ou & Singh, 2001; Mohanty & Barik) revealed that deploying a self-tuning Fuzzy PID controlled TCSC, not only improve the static stability of power system but also damped out power oscillations and enhance power stability. Validation of the works were done through MATLAB/Simulink simulation on a single and multi machine infinite bus system, that ultimately ascertain the superior efficacy of self-tuning Fuzzy PID TCSC compared to nonlinear control, conventional PID control, and fixed series compensation. Over-voltage has detrimental impact on transient stability within power system by subjecting electrical components to undue stress. It results to insulation breakdown with the potential to cause complete system blackout if not effectively managed. Several factors cause over-voltages in power system like line to ground faults, resonance conditions, load rejection, energization of transformer or combination thereof (Martinez-Velasco & Gonzalez-Molina, 2012). Sudden loss of load can lead to transient instability which compromises power quality and potentially create an imbalance between generation and consumption that results to deviation in voltage and frequency. Load rejection test conducted at a hydro power plant in Sweden to investigate the electromechanical transient processes and signal distortions deploying adaptive techniques, specifically, the Newton-Type Algorithm (NTA) and the Adaptive Fourier Filter (AFF) scheme illustrated the efficacy of the proposed adaptive methods for voltage and current measurement during high frequency variations and distortions (Rebizant & Terzija, 2003; Arastou, Karrari, & Zakar, 2021; Xiao-ming & Wei, 2017). Also, the research conducted in (Pandey & Duvvury, 2012; Arzani, Jazaeri, & Alinejad-Beromci, 2008; Litu, Heydt, & Edris, 2002; Muhammad, Chan, Li, Duan, Lei, Bo & Wagar, 2017), introduced a promising method to enhance Available Transfer Capability (ATC) through the integration of Static Synchronous Series Compensation (SSSC), TCSC, Unified Power Flow Controller (UPFC), and Interline Power Flow Controller (IPFC). The effective utilization of the FACTS devices improved the ATC of the system. The feasibility and reliability of the approach was validated by conducting a study on a modified IEEE 30 bus system using power system analysis tool box (PSAT) software and the Nigeria 58-bus power system network using NEPLAN software respectively. Studies in (Nkan, Okpo, & Okoro, Multi-Type FACTS Controllers for Power System Compensation: A Case Study of the Nigerian 48-Bus, 330Kv System, 2021; Nkan , Okoro, Awah, & Akuru, 2019; Nkan , Okoro, Awah, & Akuru, 2019; Albatsh, Mekhilef, Ahmad, Mokhlis, & Hassan, 2015) showed the synergistic effects of the combination of static VAR compensator and TCSC as opposed to using them individually. Thee research findings showed that their collective application notably diminishes real power and reactive power losses. Voltage magnitude, active and reactive power controls in the grid system were studied in (Hemeida, Hamda, Mobarak, El-Bahnasawy, Ashmaway & Senjyu, 2020; Yaghobi, 2020; Fathollahi, Kargar, & Derakhshandeh, 2022).The study deployed a novel approach by integrating TCSC with auxiliary controls to enhance voltage profiles and optimal performance in power systems the outcome showed a significant improvement in the voltage profile and the network performance. In (Nkan , Okpo, Akuru, & Okoro, 2020; Madhusudhanarao, Ramarao, & Kumar, 2010; Shah, Srivastava, & Sarda, 2016; Bhattacharyya & Kumar, 2016), an effort to improve dynamic stability and alleviate voltage limit violations, rotor angle deviations, speed fluctuations, and post-outage oscillations during line outages in the Nigeria 48-bus power network was made. A strategic integration of two FACTS (SSSC and TCSC), was conducted using PSAT in MATLAB. Another study showed an improvement in power system stability achieved through coordinated control of a FACTS device; Static VAR Compensator (SVC). Simulation was performed using both MATLAB simulation and real-time simulator tests that introduced a significant fault in the inter-area system tie-line (Dahat & Dhabale, 2023). Improved harmony search algorithm (IHS) method for optimizing SVC placement and sizing demonstrated superior performance in reducing power loses and enhancing voltage profiles compared to particle swarm optimization on a 57-bus test system (Ahmad & Sirjani, 2019). Performance evaluations with and without FACTS devices including IPFC, TCSC, and UPFC to determine the FACTS device with the best potential solution to the longstanding issues of power transfer capability in the Nigerian power system was carried out in NEPLAN, the study showed that UPFC has a better performance compared to TCSC and IPFC in significantly improving the power transfer capability of the Nigerian 58-bus network, indicating the potential for its effective application in power system enhancement (Natala, Nkan, Okoro, & Obi, 2023; Kavitha & Neela, 2018). TCSC and TCPAR were used to address contingencies in a stressed power system by reducing the line overloading to improve the overall network performance and power stability. The simulation was carried out on a modified IEEE14 bus system using PowerWorld Simulator software version 12.0 (Sayyed, Gadge, & Sheikh, 2014; Devi & Padma, 2017).

III. MODELING OF NIGERIAN 48-BUS SYSTEM WITH TCSC AND THREE PHASE FAULT

Modelling of the Nigerian 48-bus system which comprises 14 generators, 14 transformers, 51 transmission lines and 20 load buses, for transient stability with the optimum location of TCSC after application of a three phase fault at bus 33 (Geregu subatation) is illustrated with Fig. 1. This was achieved using PSAT software in MATLAB. The bus data and transmission line input data of the Nigerian power system network were picked from (Umoh, 2022).

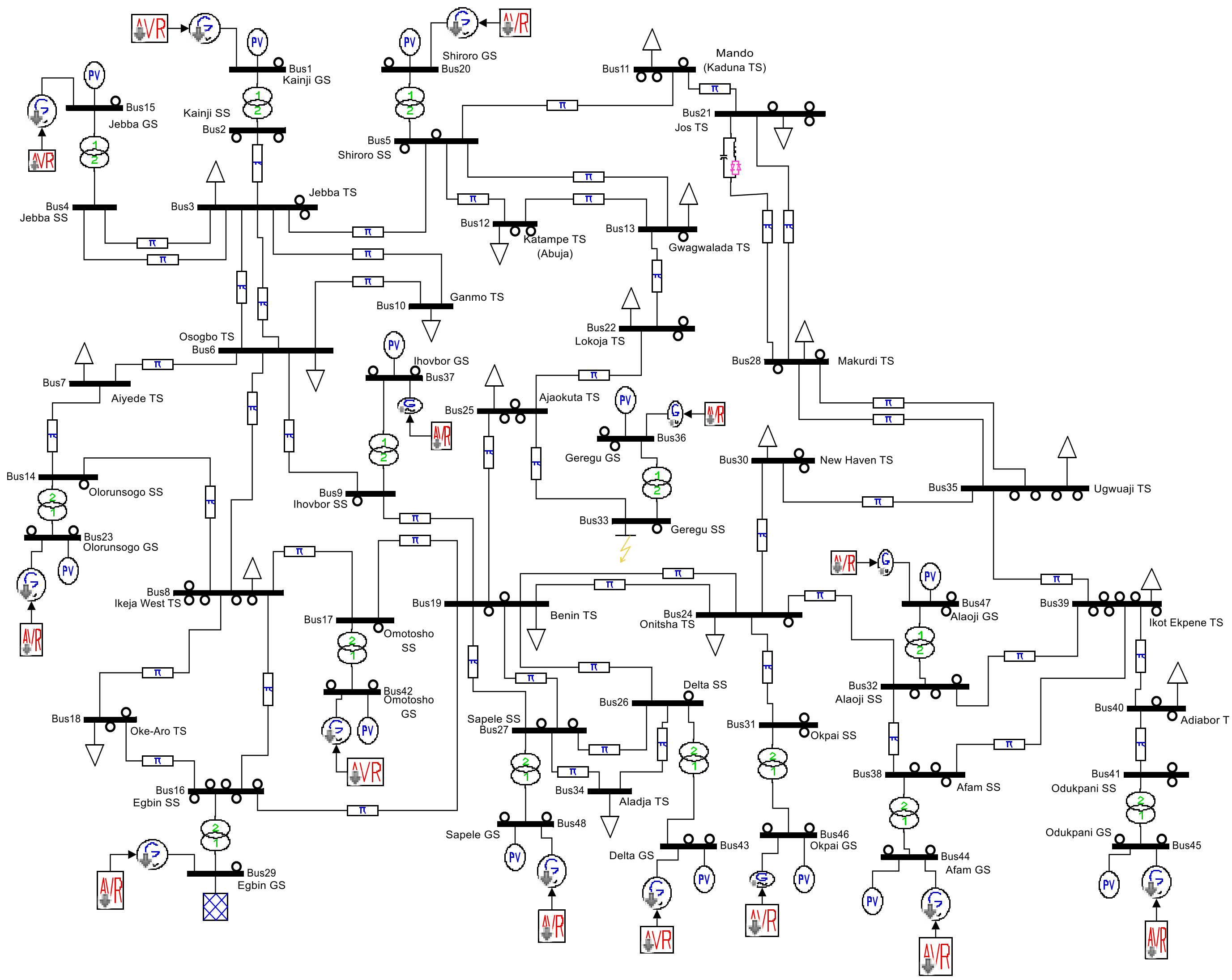

Fig. 1. Nigerian 48-bus system for transient stability studies; fault at bus 33, TCSC on line 21-28

IV. POWER FLOW MULTI-CONTROL FUNCTION WITH TCSC

The model of TCSC regulator is depicted in Fig. 2.

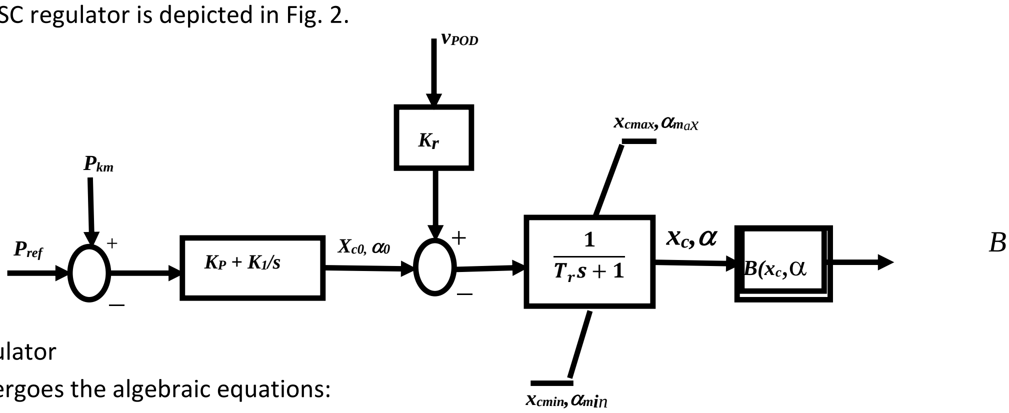

Fig. 2. TCSC regulator

The system undergoes the algebraic equations:

$$P_{km} = V_k V_m (Y_{km} + B)\sin(\theta_k - \theta_m) \tag{4.1}$$

$$P_{mk} = -P_{km} \tag{4.2}$$

$$Q_{km} = V_k^2 (Y_{km} + B) - V_k V_m (Y_{km} + B)\cos(\theta_k - \theta_m) \tag{4.3}$$

$$Q_{mk} = V_m^2 (Y_{km} + B) - V_k V_m (Y_{km} + B)\cos(\theta_k - \theta_m) \tag{4.4}$$

where the indexes k and m stand for the sending and receiving bus indices, respectively, and Y_{km} is the admittance of the line of which the TCSC is connected.

The TCSC differential equations are:

$\dot{x}_1 = (\{x_{co}, \alpha_o\} + K_{r\,VPOD} - x_1)/T_r$ (4.5)

$\dot{x}_2 = K_1(P_{km} - P_{ref})$ (4.6)

where

$\{x_{co}, \alpha_o\} = K_p(P_{km} - P_{ref}) + x_2$ (4.7)

The output signal is the series susceptance B of the TCSC, as follows:

$B(x_c) = \frac{x_c/x_{km}}{x_{km}(1-x_c/x_{km})}$ (4.8)

or

$B(\alpha) = \pi(K_x^4 - 2K_x^2 + 1)\cos K_x(\pi-\alpha)/\,[x_c(\pi K_x^4 \cos K_x(\pi-\alpha) - \pi\cos K_x(\pi-\alpha) - 2K_x^4\alpha\cos K_x(\pi-\alpha) + 2\alpha K_x^2\cos K_x(\pi-\alpha) - K_x^4\sin 2\alpha\cos K_x(\pi-\alpha) + K_x^2\sin 2\alpha\cos K_x(\pi-\alpha) - 4K_x^3 cos^2\alpha\sin K_x(\pi-\alpha) - 4K_x^2\cos\alpha\sin\alpha\cos K_x(\pi-\alpha))]$

(4.9)

$K_X = \sqrt{\frac{Xc}{XL}}$ (4.10)

During the power flow analysis, the TCSC is modeled as a constant capacitive reactance that modifies the line reactance X_{km}, as:

$x'_{km} = (1 - c_p)x_{km}$ (4.11)

where c_p is the percentage of series compensation. The TCSC state variables are initialized after the power flow analysis as well as the reference power of the PI controller P_{ref}.

V. OPTIMUM LOCATION OF TCSC USING CONTINUATION POWER FLOW

The method used in this research work to determine the bus in the Nigerian power system with the weakest voltage profile for the installation of FACTS devices is the use of the continuation power flow (CPF) technique. This is a tool embedded in PSAT for studying voltage stability performance analysis of the Nigerian power system under study. The P.V curve for each bus in the power system can be obtained using the CPF method. Continuation power flow finds successive load flow solution according to a load scenario. It consists of prediction and correction steps. From a known base solution, a tangent predictor is used so as to estimate next solution for a specified pattern of load increase. The corrector step then determines the exact solution using Newton-Raphson technique employed by a conventional power flow. After that, a new prediction is made for a specified increase in load based upon the new tangent vector. Then corrector step is applied. This process goes on until critical point is reached. The critical point is the point where the tangent vector is zero (Ajjarapu & Chriaty, 1992), as shown in Fig. 3.

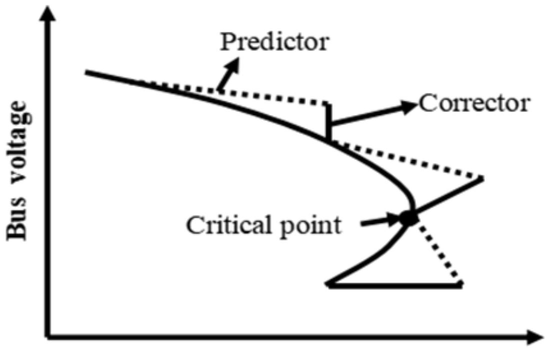

Fig. 3. Illustration of prediction-correction steps (Ajjarapu & Chriaty, 1992)

The increase in loads when the loading parameter is inserted as in the case of the dynamic system in Nigeria will cause the generators to reach their generating limits with forces tending to make such generators exceeds these limits. Since these limits cannot be exceeded, the power system will lose its voltage stability at the critical point where the load parameter is maximum. This critical point is the voltage collapse point and there is rapid decrease in the voltage magnitude as reactive power in the system is insufficient.

Injected powers can be written for the i^{th} bus of an n-bus system as follows in (5.1) to (5.3).

$P_i = \sum_{k=1}^{n}|V_i||V_k|(G_{ik}\cos Q_{ik} + B_{ik}\sin Q_{ik})$ (5.1)

$Q_i = \sum_{k=1}^{n} |V_i||V_k|(G_{ik} \sin Q_{ik} + B_{ik} \cos Q_{ik}$ (5.2)

$P_i = P_{Gi} - P_{Di}, Q_i = Q_{Gi} - Q_{Di}$ (5.3)

where the subscripts G and D denote generation and load demand respectively on the related bus. In order to simulate a load change, a load parameter λ is inserted into demand powers P_{Di} and Q_{Di}.

$P_{Di} = P_{Dio} + \lambda(P_{\Delta base})$ (5.4)

$Q_{Di} = Q_{Dio} + \lambda(Q_{\Delta base})$ (5.5)

P_{Dio} and Q_{Dio} are original load demands on i^{th} bus whereas $P_{\Delta base}$ and $Q_{\Delta base}$ are given quantities of powers chosen to scale λ appropriately. After substituting new demand powers in (4) and (5) to (3), new set of equations can be represented as:

$F(\theta,V,\lambda) = 0$ (5.6)

VI. SIMULATION RESULTS AND DISCUSSION

A. Nigerian 48-Bus at Prefault

Figs. 4-8 shows the responses of the rotor angle, rotor speed, quadrature axis (q-axis) component behind transient reactance, direct axis (d-axis) component behind transient reactance and voltage magnitude profile of the buses respectively for all the 14 generators of the Nigerian 48-bus power system network of Fig. 1 when there was no perturbation. At prefault, there was no disturbance hence, the system was relatively stable. This is depicted in all the graphs appearing in straight lines. The rotor angle of the different generators in p.u. plotted against time as shown in Fig. 4 came out as straight lines to indicate a situation of no perturbation, hence a state of stability. The same can be said of the rotor speed (Fig. 5) which has all the generators in synchronism having the same speed of 1 p.u. The q-axis and d-axis voltage component behind transient reactance (Figs. 6 and 7) depicts the various voltage levels behind transient reactance in p.u. of all the generators without disturbance hence are all in straight lines. The various voltage levels of all the 48 buses which as observed falls within the acceptable voltage limit of 0.95 to 1.05 p.u. shows a stable state without any form of disturbances hence, their straight-line form (Fig. 8)

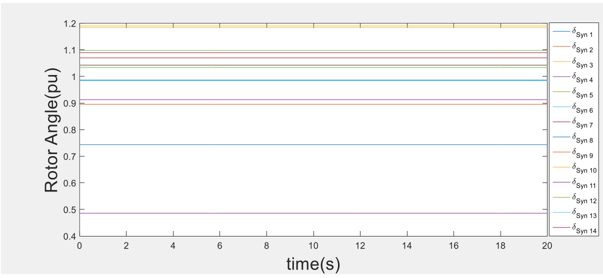

Fig. 4. Generators rotor angle responses at prefault

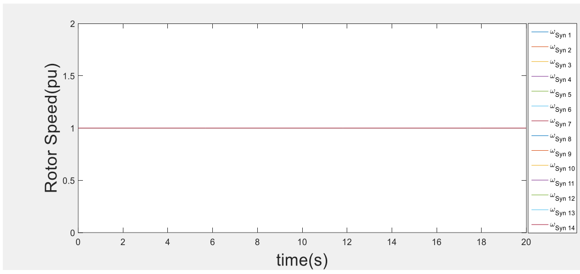

Fig. 5. Generators rotor speed responses at prefault

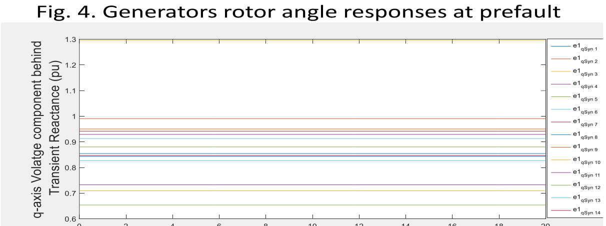

Fig. 6. Q-axis voltage component behind transient reactance responses at prefault

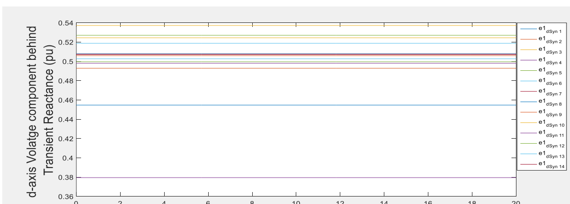

Fig. 7. D-axis voltage component behind transient reactance at prefault

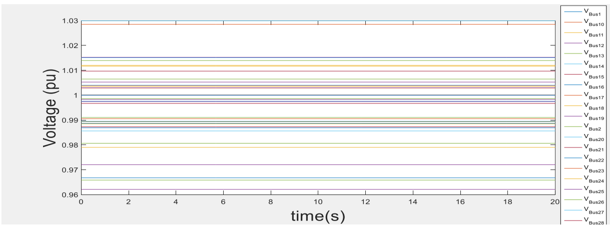

Fig. 8. Voltage magnitude profile at prefault

B. Nigerian 48-Bus System with Application of Fault

A three-phase fault with start and clearing time of 1.00s and 0.153s respectively was applied at bus 33(Geregu SS). It should be noted that the choice of the position for the application of fault was arbitrarily made since fault can occur anywhere in the system. Newton Raphson power flow simulation was performed on the system and convergence was reached after 5 iterations in 0.25s. TDS was also carried out to enhance dynamic response of the system to the fault. The DS was completed in 12.5717s on a scale of 20s. Fig. 9 illustrate the rotors angle behaviour for the fourteen synchronous generators which kept increasing until they go out of synchronism thereby loosing stability. The rotors speed which settled to steady state condition after 11.34s and whose amplitudes of swing is observed to rise up to 1.015 p.u. depending on the proximity of the generator to the fault is shown in Fig. 10. Fig. 11 shows the responses of the quadrature axis component of voltage behind transient reactance where the post fault oscillations are damped out in a much longer time. The q-axis voltage component behind transient reactance of generators 3 and 10 with p.u. voltages of 1.295 and 0.7109 respectively damped out at about 10.96s and 7.462s respectively. The amplitudes of oscillations are also seen to be high at 1.317 p.u. and 0.7647 p.u. respectively. Responses of the direct axis component of voltage behind transient reactance are displayed in Fig. 12. As observed in the q-axis component, the post fault oscillations of the d-axis voltage component behind transient reactance of generators 8 and 11 damped out at 9.837s and 9.962s respectively while the p.u. voltage swings rose up to 0.4385 and 0.4965 respectively. The result in Fig. 13 shows the voltage magnitude profile plot of all the 48 buses. Without FACTS device, the amplitude of swing is high up to 1.093 which exceeds the allowable voltage limit of 1.05. The frequency of oscillation is also high as the swing dampened out at 11.21s. This portrays a high level of instability in the system.

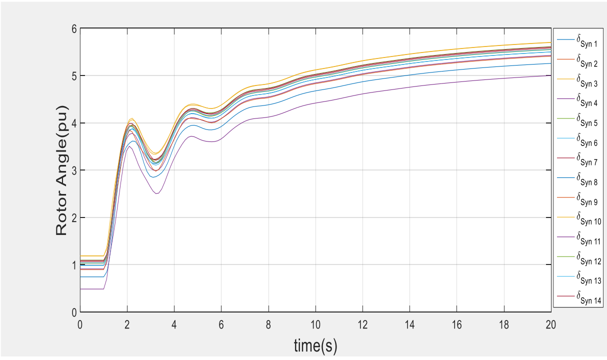

Fig. 9. Generators rotor angles, fault applied at bus 33

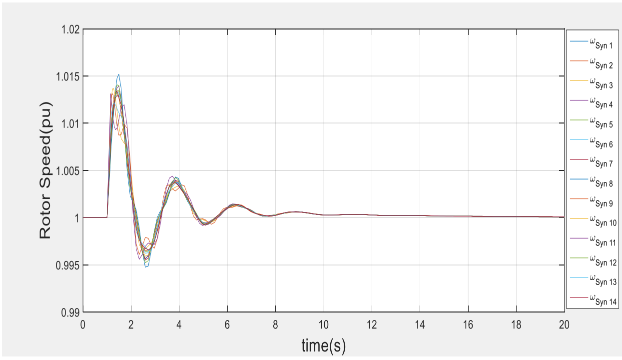

Fig. 10. Generators rotor speed, fault applied at bus 33

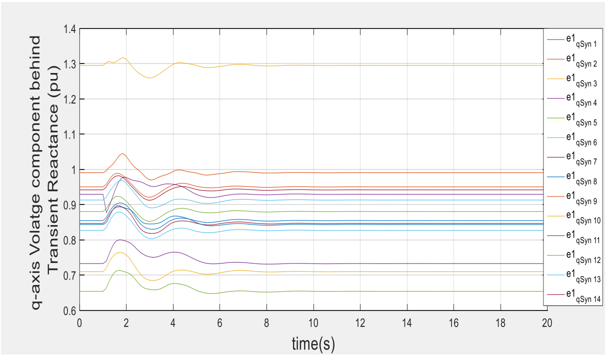

Fig. 11. Q-axis voltage component behind transient reactance responses, fault at bus 33

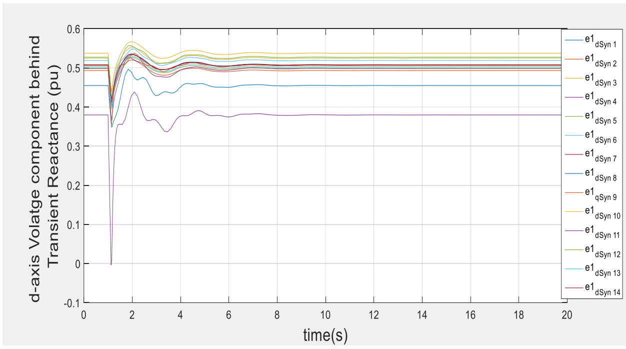

Fig. 12. D-axis voltage component behind transient reactance, fault at bus 33

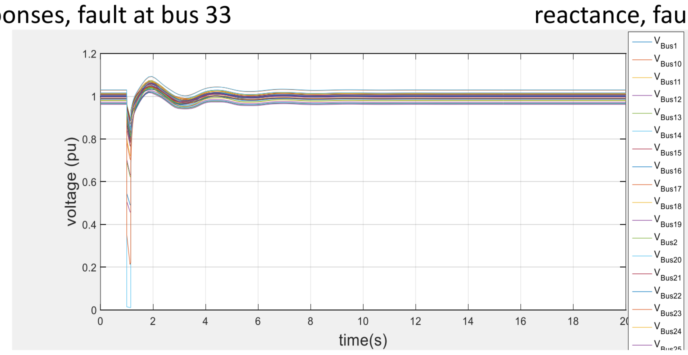

Fig. 13. Voltage magnitude profile, fault at bus 33

C. Newton-Raphson Power Flow without TCSC

Newton Raphson power flow simulation of the network of without TCSC was carried out. It was observed that in 0.187s, the stimulation converges at 1.9382$\times 10^{-9}$p.u. after 5 iterations. Time domain simulation (TDS) in PSAT embedded in MATLAB using the Trapezoidal integration method (TIM) was carried out for Transient stability analysis (TSA). Dynamic simulation (DS) was also completed in 5.8765s with maximum real and reactive power mismatch of 4.84504 p.u. and 1.95 p.u. respectively. The result of the power flow is shown in Table 1.

Table 1. Power Flow Results Of Nigerian 48-Bus System For Transient Stability Analysis

BUS NO	BUS NAME	VOLTAGE (pu)	PHASE ANGLE (rad)	REAL POWER (pu)	REACTIVE POWER (pu)
1	Kainji GS	1.0	-0.08753	2.59	0.10581
2	Kainji SS	1.0065	-0.24906	0	0
3	Jebba TS	1.004	-0.31097	-2.6	-1.19
4	Jebba SS	1.004	-0.30789	0	0
5	Shiroro SS	0.99055	-0.41357	0	0
6	Oshogbo TS	1.0117	-0.32033	-1.07	-0.56
7	Ayede TS	0.99741	-0.32876	-1.14	-0.68
8	Ikeja West TS	0.98066	-0.32636	-4.47	-1.95
9	Ihovbor SS	1.0299	-0.23366	0	0
10	Ganmo TS	1.0029	-0.32646	-1	-0.57
11	Kaduna TS	0.98933	-0.46977	-1.02	-0.51
12	Katampe TS	0.96212	-0.46539	-2.01	-1.07
13	Gwagwalada TS	0.96587	-0.45766	-1.2	-0.65
14	Olorunsogo SS	0.99758	-0.30346	0	0
15	Jebba GS	1.0	-0.16028	2.52	0.11734
16	Egbin SS	0.98686	-0.29182	0	0
17	Omotosho SS	1.0285	-0.24153	0	0
18	Okearo TS	0.97903	-0.32385	-2.2	-1
19	Benin TS	1.0153	-0.30267	-2.57	-1.08
20	Shiroro GS	1.0	-0.22184	3.02	0.44165
21	Jos TS	0.99668	-0.52377	-2.32	-1.1
22	Lokoja TS	0.96676	-0.42346	-1	-0.6
23	Olorunsogo GS	1.0	-0.20368	1.59	0.11803

24	Onitsha TS	1.0035	-0.30458	-1.8	-0.85
25	Ajaokuta TS	0.97206	-0.40232	-1.2	-0.7
26	Delta SS	1.0139	-0.27952	0	0
27	Sapele SS	1.015	-0.2883	0	0
28	Makurdi TS	1.0039	-0.46706	-1.6	-0.72
29	Egbin GS	1.0	0.0	4.845	0.93581
30	New Heaven TS	0.99847	-0.37499	-1.36	-0.77
31	Okpai SS	1.0053	-0.2647	0	0
32	Alaoji SS	0.99864	-0.2142	0	0
33	Geregu SS	0.98562	-0.3353	0	0
34	Aladji TS	1.0097	-0.29134	-1.82	-0.77
35	Ugwuaji TS	0.98946	-0.37849	-1.25	-0.69
36	Geregu GS	1.0	-0.25913	1.2	0.27584
37	Ihovbor GS	1.0	-0.08749	2.4	-0.30275
38	Afam SS	0.99825	-0.20542	0	0
39	Ikot Ekpene TS	0.99105	-0.23741	-1.65	-0.74
40	Adiabor TS	0.98728	-0.20438	-0.9	-0.48
41	Odukpani SS	0.98869	-0.19134	0	0
42	Omotosho GS	1.0	-0.12704	1.88	-0.34825
43	Delta GS	1.012	-0.10752	2.81	0.21084
44	Afam GS	1.003	-0.02974	2.8	0.32277
45	Odukpani GS	1.0	-0.02624	2.6	0.39616
46	Okpai GS	1.0	-0.12687	2.21	0.06808
47	Alaoji GS	1.0	-0.06343	2.4	0.20311
48	Sapele GS	1.0	-0.18743	1.7	-0.15135

D. Optimum Location of TCSC

Continuation power flow was carried out on the system in order to determine the weakest bus for the installation of TCSC device. The simulation was completed in 1.3835s with maximum loading parameter (λmax) = 1.6592. Table 2 shows the results of CPF where buses 11(Kaduna Ts), 12(Katampe TS), 13(Gwagwalada TS), 21(Jos TS), 22(Lokoja TS), 25(Ajaokuta TS), 28(Makurdi TS), 30(New Heaven TS) and 35(Ugwuaji TS) were found to be very weak buses with voltages well below 0.8 p.u. as highlighted. Graphical representation of this voltage profile is shown in Fig. 14 and the outcome indicates that bus 21(Jos TS) is the weakest bus with voltage magnitude of 0.54149 p.u. To confirm the above results, a plot of the P–V curves (variation of bus voltage with loading factor) was generated for the lowest voltage buses. This is illustrated in Fig. 15. The figure shows the changes in the bus voltage with increase in the loading parameter lambda (l) for the Nigerian 48-bus system. The plots of buses 11, 12, 13, 21, 22, 25, 28, 30 and 35 shows that bus number 21 is the most insecure as the voltage of each reactive load of bus 21 is the least. This affirms the best location for the installation of the TCSC FACTS device for power system stability enhancement.

Table 2. Continuation Power Flow Results Of The Nigerian 48-Bus System Fortransient Stability Analysis

BUS NO	BUS NAME	VOLTAGE (p.u.)	PHASE ANGLE (rad)	REAL POWER (p.u.)	REACTIVE POWER (p.u.)
1	Kainji GS	1.0	-0.3068	4.2972	1.2306
2	Kainji SS	0.95822	-0.40975	0	0
3	Jebba TS	0.92027	-0.52063	-4.3138	-1.9744
4	Jebba SS	0.924	-0.51516	0	0
5	Shiroro SS	0.8188	-0.844	0	0
6	Oshogbo TS	0.91388	-0.51198	-1.7753	-0.92913
7	Ayede TS	0.90281	-0.49124	-1.8915	-1.1282
8	Ikeja West TS	0.86832	-0.41292	-7.4165	-3.2354
9	Ihovbor SS	0.9542	-0.4016	0	0
10	Ganmo TS	0.90563	-0.53914	-1.6592	-0.94573
11	**Kaduna TS**	**0.69135**	**-1.0134**	**-1.6924**	**-0.84618**
12	**Katampe TS**	**0.73763**	**-0.9794**	**-3.3349**	**-1.7753**
13	**Gwagwalada TS**	**0.74688**	**-0.95828**	**-1.991**	**-1.0785**
14	Olorunsogo SS	0.92935	-0.4117	0	0
15	Jebba GS	1.0	-0.41633	4.1811	2.6517
16	Egbin SS	0.89274	-0.29937	0	0
17	Omotosho SS	0.81462	-0.76092	-7.4165	-3.2354
18	Okearo TS	0.87299	-0.38693	0	0
19	Benin TS	0.91584	-0.5949	-4.2641	-1.7919
20	Shiroro GS	1.0	-0.72498	5.0107	6.9887
21	**Jos TS**	**0.54149**	**-1.2887**	**-3.8493**	**-1.8251**
22	**Lokoja TS**	**0.76864**	**-0.87242**	**-1.6592**	**-0.9955**
23	Olorunsogo GS	1.0	-0.33709	2.6381	2.0155

24	Onitsha TS	0.89512	-0.60818	-2.9865	-1.4103
25	**Ajaokuta TS**	**0.79118**	**-0.82062**	**-1.991**	**-1.1614**
26	Delta SS	0.97175	-0.55948	0	0
27	Sapele SS	0.94283	-0.57117	0	0
28	**Makurdi TS**	**0.61286**	**-1.0608**	**-2.6547**	**-1.1946**
29	Egbin GS	1.0	0	15.1641	5.9032
30	**New Heaven TS**	**0.74694**	**-0.77106**	**-2.2565**	**-1.2776**
31	Okpai SS	0.96846	-0.54106	0	0
32	Alaoji SS	0.97449	-0.44856	0	0
33	Geregu SS	0.88899	-0.67922	0	0
34	Aladja TS	0.95446	-0.5798	-3.0197	-1.2776
35	**Ugwuaji TS**	**0.73874**	**-0.78035**	**-2.074**	**-1.1448**
36	Geregu GS	1.0	-0.56742	1.991	1.9835
37	Ihovbor GS	1.0	-0.13423	3.982	0.35109
38	Afam SS	0.9805	-0.43422	0	0
39	Ikot Ekpene TS	0.93647	-0.48663	-2.7376	-1.2278
40	Adiabor TS	0.97182	-0.43344	-1.4933	-0.7964
41	Odukpani SS	0.98586	-0.41291	0	0
42	Omotosho GS	1.0	-0.56784	3.1192	2.6841
43	Delta GS	1.012	-0.52795	4.6623	4.6927
44	Afam GS	1.003	-0.40181	4.6465	2.4611
45	Odukpani GS	1.0	-0.39293	4.3138	2.3911
46	Okpai GS	1.0	-0.51582	3.6668	3.6064
47	Alaoji GS	1.0	-0.42135	3.982	2.9262
48	Sapele GS	1.0	-0.40482	2.8208	0.46255

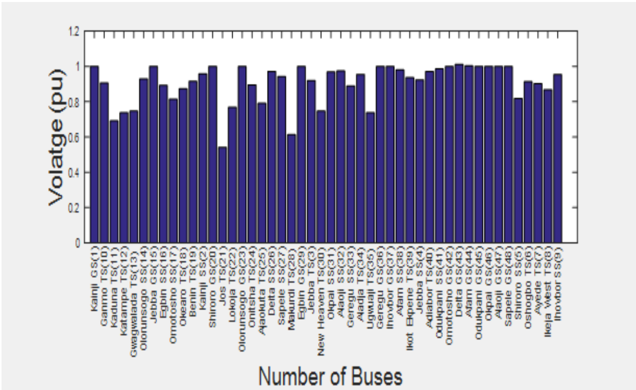

Fig. 14. Voltage magnitude profile after CPF for transient stability analysis

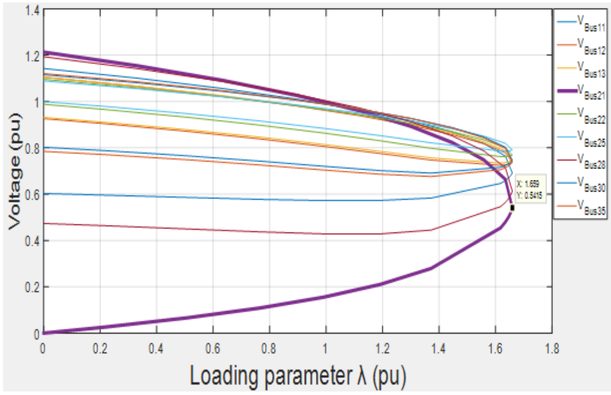

Fig. 15 Voltage P-V nose curves for nine low voltage buses

E. Power Flow Simulation with TCSC

Following the perturbation of the system when a three-phase fault was applied to system, starting at 1.00s and cleared after 0.153s at bus 33(Geregu SS), the system was observed to be unstable as was seen in the characteristics responses of the various system parameters (Figs. 16-20). TCSC was optimally placed in the system on line 21–28 very close to the weakest bus 21(Jos TS). Power flow simulation was performed on the system and after 5 iterations in 0.218s, convergence was reached with maximum convergence error of 1.2389 p.u. TDS was also carried out to enhance dynamic responses of the system. The DS was completed in 14.5231s on a scaled stimulation time of 20s.

Fig. 16 displays the generator 6 rotor angle response with and without the installation of TCSC. The response clearly displays the compensation capability of TCSC in the reduction of the rotor angle whereas the system without TCSC shows the increment of the rotor angle with time until steady-state is restored after clearing time. Fig. 17 depicts the generator 6 rotor speed response with TCSC and without TCSC. The post fault settling time with TCSC is observed to be about 7.712s compared to the 11.71s without TCSC device. It can also be seen clearly that the maximum displacement of the oscillation is greater without TCSC at 1.013 p.u. compared to the system with TCSC which oscillate about its reference value of 1.0 p.u. The response of the q-axis voltage component behind transient reactance for generator 6 with TCSC is represented in

Fig. 18. It is noticed that post fault oscillation of the system with TCSC damped out faster at 6.837s than the system without TCSC at 11.09s respectively. The amplitude of swing without TCSC is high at about 0.0523 p.u. compared to the system with TCSC which oscillate about its reference value of 0.8866 p.u. The same can be said concerning the d-axis voltage component behind the transient reactance displayed in Fig. 19. The amplitude of swing without TCSC is very high with a dip of about 0.3944 p.u. whereas the system with TCSC oscillates about its reference value. The post fault oscillation settling time is less with the system with TCSC which stands at 6.587s compared to 10.09s of the system without TCSC. Fig. 20 illustrates the voltage magnitude profile with and without TCSC for generator 6. It is observed that the post fault amplitude of oscillation of the system without TCSC is very high above the upper allowable limit of 1.05 p.u. As observed, it stands at 1.06 p.u. It also took a dip to about 0.8368 p.u as against the acceptable lower limit of 0.95 p.u. The system with TCSC oscillate less and damped out faster in 4.712s compared to 9.964s without TCSC.

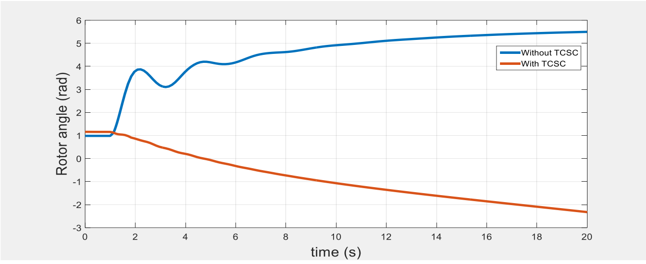

Fig. 16. Generator 6 rotor angle response with and without TCSC; fault at bus 33

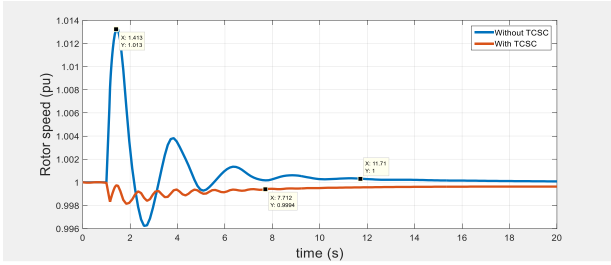

Fig. 17. Generator 6 rotor speed response with and without TCSC; fault at bus 33

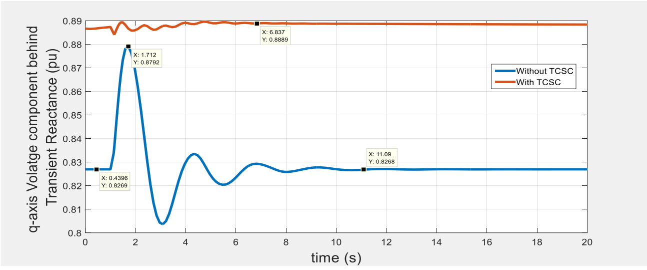

Fig. 18. Generator 6 q-axis voltage component behind transient reactance response with and without TCSC; fault at bus 33

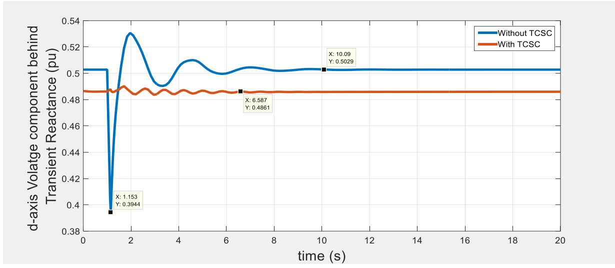

Fig. 19. Generator 6 d-axis voltage component behind transient reactance response with and without TCSC; fault at bus 33

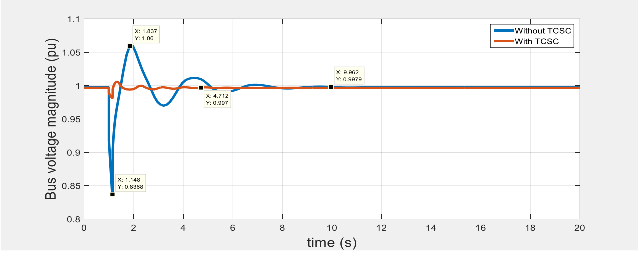

Fig. 20 Generator 6 Voltage magnitude profile with and without TCSC; fault at bus 33.

VII. CONCLUSION

Effects of TCSC, a series FACTS controller has been optimally positioned in the Nigerian 48- bus system using continuation power flow for transient stability enhancement. These effects were seen in the responses of the synchronous generators' rotor angle, rotor speed, quadrature axis and direct axis voltage component behind transient reactance as well as the voltage magnitude profile to the contingency of an incidental fault on bus 33 at Geregu substation and TCSC optimally placed on line 21-28. Simulation results showed the magnificent reduction in the post fault oscillation time as the oscillation damped out much faster and the voltage profile was improved for transient stability with the installation of FACTS controllers.

REFERENCES

1) Pandey R. K and Duvvury C.V 2012. Ahmad, A. A., & Sirjani, R. (2019). Optimal placement and Sizing of Multi-type FACTS Devices in Power Systems using Metaheuristic Optimization Technique: An Updated Review. Ain Shams Engineering Journal, 2090- 4479. doi:10.1016/j.ase.2019.10.013
2) Ajjarapu, E., & Chriaty, C. (7). The Continuation Power Flow: A Tool for Steady State Stability Analysis. IEEE Transaction on Power System , 7(1), 416-423.
3) Albatsh, F. M., Mekhilef, S., Ahmad, S., Mokhlis, H., & Hassan, M. A. (2015). Enhansing power transfer cability through flexible AC transmission system devices: a review. Frontier of Information and Electronic Engineering , 16, 658-678.
4) Arastou, A., Karrari, M., & Zakar, B. (2021). New method for Synchronous Generator Parameters Estimation Using Load Rejection Tests Data Considering Operational Limitations . ScienceDirect, 192.
5) Arzani, A., Jazaeri, M., & Alinejad-Beromci, Y. (2008). Available transfer capability enhancement using series FACTS devices in a designed multi machine power system . 43rd International Universities Power Engineering Conference . Padua, Italy.

6) Bhattacharyya, B., & Kumar, S. (2016). Loadability Enhancement with FACTS Devices using Gravitational Search Algorithm. Electrical Power and Energy System, 78, 470-479.7)Dahat, S. A., & Dhabale, A. (2023). Rotor angle stability improvement by coordinated control of SVC and SSSC controllers. The 3rd International Conference on Power and Electrical Engineering (ICPEE 2022), 9, pp. 13-22. Singapore.
7) Devi, A. H., & Padma, S. (2017). Optimal Location and Parameter Setting of FACTS Devices based on WIPSO and ITLBO for Power System Security Enhancement under Single Contingency. International Journal of Engineering and Advance Technology (IJEAT) , 6(6).
8) Fathollahi, A., Kargar, A., & Derakhshandeh, S. Y. (2022). Enhancement of power system transient stability and voltage regulation performance with decentralized synergetic TCSC controller. International Journal of Electrical Power and Energy Systems, 135.
9) Hemeida, A. M., Hamada, M. M., Mobarak, Y. A., El-Bahnasawy, A., Ashmawy, M. G., & Senjyu, T. (2020). TCSC with auxiliary controls based voltage and reactive power contols on grid power system . ScienceDirect, 11(3), 587-609.
10) Hingorani, N. G. (2000). Role of FACTS in a deregulated market. Power Esngineering Society Summer Meeting (Cat. No. 00CH37134), 3, pp. 1463-1467. Seattle, WA, USA,.
11) Karthiga, M. M., Raja, S. C., & Venkatesh, P. (2017). Enhancement of available transfer capability using TCSC ddevices in deregulated Power Market. Inniovation in Power and Advance Computing Technologies (i-PACT) , (pp. 1-7). Velloere, India.
12) Kavitha, K., & Neela, R. (2018). Optimal allocation of multi-type FACTS devices and its effect in enhancing system security using BBO, WIPSO and PSO . Journal of Electrical Systems and Information Technology, 5(3), 777-793.
13) Litu, C.-C., Heydt, G. T., & Edris, A. A. (2002). Impacts of FACTS Controllers on Transfer Capability of Power grids . IEEE Power Engineering Society Winter Meeting. Conference Proceedings (Cat.No.02CH37309), (pp. 556-561). Newyork, NY,USA.
14) Madhusudhanarao, G., Ramarao, P. V., & Kumar, T. J. (2010). Optimal Location of TCSC and SVC for enhancement of ATC in a de-regulated environment using RGA. IEEE International Conference on Computational Intelligence and Computing Research. Coimbatore, India.
15) Martinez-Velasco, J. A., & Gonzalez-Molina, F. (2012). Temporary Overvoltage in Power Systems . In Power Systems Transients (p. Chapter 5). United Nations: The Encyclopedia of Life Support Systems (EOLSS).
16) Mohanty, K. A., & Barik, K. A. (n.d.). Power System Stability Improvement Using FACTS Devices. International Journal of Modern Engineering Research (IJMER), 1(2), 666-672.
17) Muhammad, Z., Chen, J., Li, Y., Duan, X., Lei, Q., Bo, W., Waqar, A. (2017). New Approach for Optimal Location and Parameter Setting of UPFC for Enhancing Power Systems Stability under Contingency Analysis. Energies, 10(11).
18) Natala, H., Nkan, I. E., Okoro, O., & Obi, P. I. (2023). Investigation of the Transfer Capability of the Nigerian 330kV, 58-bus Power System Network using FACTS Devices . ELEKTRIKA-Journal of Electrical Engineering , 22(1), 53-62.
19) Nkan, I. E., Okoro, O. I., Awah, C. C., & Akuru, U. B. (2019). Investigating the Dynamic Stability of the Nigerian 48-Bus Systems for Improved System Performance using FACTS. Proceedings of the 27th Domestic use of Energy Conference.
20) Nkan, I. E., Okoro, O. I., Awah, C. C., & Akuru, U. B. (2019). Investigating the Steady State Stability of the Nigerian 48-Bus Systems using FACTS Devices. Nigerian Journal of Technology (NIJOTECH), 38(3), 732-743.
21) Nkan, I. E., Okoro, O. I., Obi, P. I., Awah, C. C., & Akuru, U. B. (2019). Application of FACTS Devices in a Multi-Machine Power System for Transient Stability Enhancement: A Case Study of the Nigerian 330kV 48-Bus System . IEEE AFRICON, (pp. 1-9). Accra, Ghana.
22) Nkan, I. E., Okpo, E. E., & Okoro, O. I. (2021). Multi-Type FACTS Controllers for Power System Compensation: A Case Study of the Nigerian 48-Bus, 330Kv System. Nigerian journal of Technological Development, 18(1), 63-69.
23) Nkan, I. E., Okpo, E. E., Akuru, U. B., & Okoro, O. I. (2020). Contingency Analysis for Improved Power System Stability of the Nigerian 330Kv, 48-Bus System using Series FACTS Controllers. AIUE Congress 2020: International Conference on Use of Energy.
24) Ou, Y., & Singh, C. (2001). Improvement of total transfer capability using TCSC and SVC . Power Engineering Society Summer Meeting.Conference Proceedings (Cat. No. 01CH37262). Vancouver, BC, Canada.
25) Pandey, R. K., & Duvvury, C. V. (2012). An effective appproach for ATC enhancement with FACTS device - A case study. International Conference on Advances in Power Conversion and Energy Technologies (APCET), (pp. 1-6). Mylavaram, India.

26) 27) Rebizant, W., & Terzija, V. (2003). Asynchronous generator behaviour after a sudden load rejection . IEEE Bologna Power Tech Conference Proceedings , 2, p. 7. Bologna, Italy .
27) Sayyed, A. n., Gadge, P. M., & Sheikh, R. U. (2014). Contingency Analysis and Improvement of Power System Security by Locating Series FACTS Devices "TCSC and TCPAR" at Optimal Location . International Conference on Advances in Engineering and Technology (ICAET-2014).
28) Shah, I., Srivastava, N., & Sarda, J. (2016). Optmal Placement of multi-type facts controllers using real coded genetic algorithm . International Conference on Electrical, Electronics, and Optimization Techniques(ICEEOT) . Chennai, India.
29) Sunikumar, P. (2012). Transient Stability Enhancement of Power System Using TCSC. International Journal of Electrical and Computer Engineering (IJECE), 2(3), 317-324.
30) Umoh, E. C. (2022). Top of the Hour Maximum Power Flow of the Grid 330kV Daily Load Flow. National control Center Oshogbo (Transmission Company of Nigeria).
31) Xiao-ming, W., & Wei, Z. (2017). Study of Synchronous Generator Parameters Test and Method of Identification. 3rd International Conference on Intelligent Energy and Power System (IEPS 2017). Nanning, China.
32) Yaghobi, H. (2020). Transient stability enhancement of power system with instability tolerant synchronous generator. The Institute of Engineering and Technology, 14(21), 4654-4665.